Two-Stage Successive Wyner-Ziv Lossy Forward Relaying for Lossy Communications: Rate-Distortion and Outage Probability Analyses

Tadashi Matsumoto, Amin Zribi, Reza Asvadi, Elsa Dupraz, Wensheng Lin

Two-Stage Successive Wyner-Ziv Lossy Forward Relaying for Lossy Communications: Rate-Distortion and Outage Probability Analyses

Tad Matsumoto, *Life Fellow, IEEE*, Amin Zribi, *Senior Member, IEEE,* Reza Asvadi, *Senior Member, IEEE,* Elsa Dupraz, *Member, IEEE,* Wensheng Lin, *Member, IEEE*

***Abstract*—This paper presents in-depth rate-distortion and outage probability analyses for two-stage successive Wyner-Ziv (WZ) wireless communication networks. The system model assumes Lossy Forward (LF) cooperative communication where lossless reconstruction is not necessarily required at the relay. This paper aims to quantitatively derive the relationship in distortions between the Source-to-Destination and the Source-to-Relay links. Hence, the design parameters are the distortion levels at the relay and destination. The admissible rate-distortion regions are first analyzed for the two stages separately, where the relay is referred to as Helper. The rate constraints with the links involved in the end-to-end (E2E) communications are then derived. Distortion Transfer Function (DTF) is introduced as a mathematical tool for analyzing the distortions of networks having multiple stages. It is shown that the higher the correlation between the Source and Helper observations, as well as the larger the E2E tolerable distortion, the larger the admissible rate region. The outage probability of the two-stage successive WZ system is evaluated, assuming that the second stage suffers from block Rayleigh fading while the first stage performs over a static wireless channel. The E2E outage probability is also analyzed with the distortion requirements at Helper and Destination as parameters in independent and correlated fading variations. It is demonstrated that the decay of the outage probability curve exhibits a second-order diversity in a low-to-medium value range of average signal-to-noise ratios (SNRs) when the helper distortion is relatively low. It is shown, however, that as long as the reconstruction at Helper is lossy, the outage probability curve asymptotically converges to the decay corresponding to the first-order diversity at high average SNRs.**

***Index Terms*—Lossy communications, lossy forward relaying, outage probability, rate-distortion analysis, Wyner-Ziv problem.**

Corresponding author: Wensheng Lin.

This work is supported in part by French National Research Agency Future Program under reference ANR-10-LABX-07-01, in part by National Natural Science Foundation of China under Grant 62001387, in part by the Young Elite Scientists Sponsorship Program by the China Association for Science and Technology under Grant 2022QNRC001.

T. Matsumoto is with IMT Atlantique Bretagne Pays de la Loire, 4 Rue Alfred Kastler, 44300 Nantes, France, and also with the Centre for Wireless Communications, University of Oulu, 90014 Oulu, Finland (e-mail: tadashi.matsumoto@imt-atlantique.fr).

A. Zribi is with the ICT Department of ISETCom, Ariana, Tunisia, and also with IMT Atlantique Bretagne Pays de la Loire, 29238 Brest, France (e-mail: amin.zribi@isetcom.tn).

R. Asvadi is with the Department of Telecommunications, Faculty of Electrical Engineering, Shahid Beheshti University, Tehran 1983963113, Iran (e-mail: r_asvadi@sbu.ac.ir).

E. Dupraz is with the Lab-STICC, IMT Atlantique, Université Bretagne Loire (UBL), 29238 Brest, France (e-mail: elsa.dupraz@imt-atlantique.fr).

W. Lin is with the School of Electronics and Information, Northwestern Polytechnical University, Xi'an, Shaanxi 710129, China (e-mail: linwest@nwpu.edu.cn).

I. Introduction

Our legacy wireless communications systems have evolved to support the demands for growing user density and flexibility in providing various applications. The forthcoming wireless networks, such as Beyond-5th generation (B5G) and 6th generation (6G) Systems, are anticipated to integrate various types of applications. One important category of these networks is identified as Cellular Vehicle-to-X communication (C-V2X) [1], [2] systems which range from conventional mobile communications and the Internet-of-Things (IoT), to more complex data exchange services. A widely accepted concept for the next generation systems is that sensing, communications and decision-making processes are unified into a single network supporting complex data exchange as in [3], [4]. Consequently, the system components for these three processes should be designed jointly to satisfy end-to-end (E2E) quality requirements of various applications.

A general view of wireless networks following the concept described above is that there are massively distributed sensing and communicating nodes which aim to transmit the sensed data cooperatively to achieve accurate final decisions. The sensing phase relies on heterogeneous information captured by the distributed sensors which provide *correlated* sensing information. The wireless network comprises distributed nodes with cooperative communication capability, which aims to provide data forwarding with the *necessary level of reliability* for final decision-making [5]. In many applications with stringent latency requirements and limited resources, the decision-making process may be handled at the network edge to make *fast* tentative decisions. Furthermore, it should be noted that the system performance often depends on the probability of making correct decisions, even if the sensed observation can not be properly reconstructed. This shifts the system design paradigm from lossless to lossy communications, where the destination (Destination) can accept a certain level of distortion due to lossy data compression or error-prone data transmission. Recently, emphasis has been set on the lossy communication framework in smart grid networks [6], micro-robots [7] and vehicle platooning [8]. A separated role division concept is adopted in the contributions [6]–[8] where the communication part aims to transmit the sensing data obtained by multiple sensors with very low latency. In contrast, the decision-making process aims to achieve very reliable final decisions from the received lossy data. With this concept, the communication

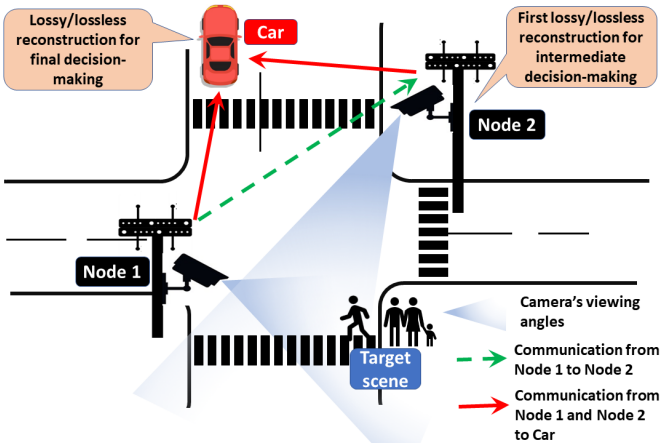

Fig. 1. Example of communication scenario involving two stages of correlated lossy source transmission with tentative decision-making at the helping node and final decision-making at Car.

part should not necessarily be lossless, and the decision-making part utilizes sophisticated machine learning (ML) and/or artificial intelligence (AI) techniques [9] over the lossy reconstructed information. Moreover, by leveraging AI/ML at the network edge, decision-making nodes proactively use their local predictions, aiming to eventually achieve zero-latency [10]. According to this concept, the tolerable distortion level is the Quality-of-Service (QoS) requirement set by the decision maker to the communication network. Therefore, this paper focuses on lossy wireless cooperative communication networks where correlated observations obtained by multiple nodes at the sensing phase are transmitted to Destination under fixed requirements on the E2E distortion level. The communication network is called lossless, with the E2E distortion requirement set to zero.

Fig. 1 shows a practical autonomous vehicle driving scenario where two cameras are equipped with two wireless communication devices on the road sides, one with Node 1 and the other with Node 2. Since the two cameras capture the road traffic from different angles in this scenario, their observations are correlated. The information representing the sensed view of the target scene, obtained by the camera at Node 1, is transmitted directly to Destination, Car, and also to Node 2. The latter works as a relay (Relay), also referred to as Helper in this paper. Helper makes an intermediate reconstruction which may be lossless or lossy, by utilizing the information obtained by its camera as well as the information transmitted from Node 1. Node 2 then makes a tentative decision utilizing the reconstruction of the target scene. The role of Node 2 is also to relay the reconstructed information to Destination. Therefore, the latter receives two versions of the original scene, one from Node 1 and the other from Node 2, which are correlated. Orthogonal signaling is assumed for the signal transmissions over the component networks at the first and the second stages .

Summarizing the roles of the cooperative network with Node 1, Node 2 and Destination described above, the network has two objectives: (1) Node 2 makes an intermediate reconstruction of the scene for tentative decision-making, and (2) Destination aims to make a full reconstruction for the final decision. However, the reconstructions by both Node 2 and Destination may be lossy or lossless. In the lossy case, the distortion requirement is defined from the decision-making process. The wireless networks having the objectives (1) and (2) can all be categorized as distributed multi-terminal coding problem. Furthermore, the roles of (1) and (2) played successively by the first and the second stages, respectively, can be formulated according to the framework of the Wyner-Ziv (WZ) problem [11]. Therefore, the utilized model in this paper can be assumed as a two-stage successive Wyner-Ziv system.

Distributed multi-terminal lossy/lossless coding represents a crucial and fundamental subject which appeared half a century ago in the field of Information and Communication Theory [12]. Originally, Slepian and Wolf (SW) identified the admissible rate region for lossless reconstruction of the multiple correlated sources [13]. The concept is now utilized in the lossy forward (LF) relaying techniques [14]–[19] with application to mobile wireless communications. In the LF research framework, since the original information and its relayed version are correlated even in the presence of transmission errors occurring in the links, they are used to reconstruct the original information at Destination losslessly. Hence, the system setup can be analyzed by utilizing the Slepian-Wolf theorem. Since Destination is only interested in the lossless reconstruction of the information sent from the source (Source), Relay works as Helper and provides side information to Destination. Of course, the shape of the admissible rate region changes depending on the mutual information between the reconstructed information at Relay and Destination [11]. However, since in mobile wireless communications the channels conditions vary according to the fading variation, the shape of the admissible rate region also exhibits time-varying nature. In [14], the outage probability of the LF relaying system is investigated in Rayleigh fading channels. Moreover, [15]–[19] apply LF relaying to other network topologies and propagation scenarios. LF relaying was also investigated in a system with simultaneous wire- less information and power transfer (SWIPT) capability [20]. Authors in [21] derived the outage probabilities and outage capacities of SWIPT based three-step two-way decode-and-forward (DF) relay networks. Recently, Ref. [22] focused on intelligent reflecting surface (IRS)-assisted sidelink transmission systems, and showed that, under block Rayleigh fading, LF relaying is more efficient than DF, especially when the number of IRS elements is small.

Distributed multi-terminal lossy coding is an extension of the lossless case; the rate-distortion (RD) functions in this case are analyzed in [23]–[25]. Wyner and Ziv derived the rate-distortion region for the distributed lossy source coding problem with side information at the decoder [23]. Berger [24] and Tung [25] determined inner and outer bounds of the achievable RD region of multi-terminal source coding with two sources. In [26], the RD function is analyzed with quadratic Gaussian Chief Executive Officer (CEO) problem. Ref. [27] proposed a modified Berger-Tung coding by changing the constraints of codebook design for Federated Learning applications where data sharing is replaced with model sharing. As in the lossless

case, the information theoretic results [23]–[26] are utilized in [28] where the LF technique is used in E2E lossy cases. The trade off between tolerable maximum distortion, rate constraints, and outage probability of the system is analyzed in [28]. It is then shown that in fading channels, the higher the tolerable distortion at Destination, the larger the rate-distortion region, yielding lower outage probability. Recently, it is shown in [29] that the outage probability with a lossy one-source one-helper Wyner-Ziv system over fading Multiple Access Channels (MACs) is larger than that over two-phase fading orthogonal transmissions, but the difference is very slight. This result provides very meaningful insight that MAC transmission is useful to reduce the transmission latency without sacrificing the system outage significantly if the source information is not necessarily reconstructed at Destination. The outage probability of two source transmission assisted by a single optimal Helper is derived in [30] by applying the admissible RD region with multi-terminal source coding [24]. It is shown in [30] that larger admissible RD region can be achieved by a single optimal Helper, yielding lower outage probability. Moreover, the latency of lossy communications with two correlated sources is studied in [31] using Gaussian codebooks and average Age-of-Information (AoI) is derived with system outage probability as a parameter. The study [31] has been further extended in [32] to the case where an analytical framework of the upper bound on average AoI in systems with the first-come-first-served scheme is established.

Notice that none of the previous contributions summarized above covers the case where both Source and Relay have their observations of the same target, as exemplified by Fig. 1. Such system can be viewed as distributed lossy and/or lossless transmission of correlated sources via two successive stages, as

- In the first stage, the problem can be seen as a WZ system where Source (Node 1) transmits the sensed information to Helper (Node 2). The latter has its own sensing information which is used as the side information.
- The second stage can also be seen as a WZ system where, Destination (Car) receives the information transmitted from Source and the side information sent from Helper.

The primary objective of this contribution is to extend the major results of [28] to a two-stage WZ system where lossy source reconstructions at both Helper and Destination are aimed at. These losses affect the accuracy of tentative and final decisions, respectively, and the maximum tolerable distortions at the two nodes are set as parameters. The E2E distortion is regarded as the decision makers' quality requirements imposed on the communication part[1,2]. The maximum tolerable distortion at Relay is specified as a constraint when critical decisions have to be made intermediately. In this case, the first stage should be considered independent of the two-stage WZ system. However, if the requirement is the E2E distortion, we must analyze the two stages jointly. It is shown in Section III.B that the distortion transfer function (DTF) denoted as $\Lambda(.,.)$ having two variables, derived by utilizing the mathematical properties of the binary convolution, plays an important role when analyzing the successive WZ problem.

In this work, it is assumed that the correlation between the observations by Source and Helper is represented by a bit-flipping model with a fixed flipping probability, as the one in [33]. Since Destination is moving, the transmission links for the wireless transmissions with the second stage suffer from fading. In this paper, we assume that the velocity of the Destination is less than a threshold, such that the block length is short enough compared to the fading coherence time[3]. Hence, the frequency-flat block fading model [35] is adopted, as in [19], [29], [36], and determining the threshold is out of the scope in this paper. The outage event is defined as the case where the rate pair supported by the wireless transmission links falls outside the admissible RD region. The outage probability is then calculated theoretically by a two-fold area integral with respect to the two probability density functions (PDFs) over the range defined by the rate region. This paper first derives the theoretical expression of the outage probability, and then shows the numerical results of the outage curves. Since the Monte-Carlo method [37] is shown to well match the theoretical results with respect to numerical integral calculations of the outage probability [14], this paper also relies on the Monte-Carlo method to obtain the numerical results for the area integral. The major contributions of this paper are summarized as follows.

i) This paper derives the admissible RD region for a two-stage successive WZ system for binary sources. The proposed DTF takes advantage of the binary convolution property, and recursively utilizes the connection between its function value and the associated argument variables. The DTF works as a *bridge* from the first to the second WZ stages, enabling the theoretical analysis of the entire system as a whole.

ii) Based on the derived admissible RD regions of the two-stage WZ system, we calculate the outage probability in block Rayleigh fading where the impact of distortion requirements at Helper and Destination is taken into account. We further analyze how the tolerable distortions with the two stages are related and how significant is their impact on the system outage probability. Conversely, given the outage probabilities fixed, how the tolerable distortions are allocated to the first and second stages is

[1]This paper focuses on the communications part only. The decision-making part may largely rely on the most advanced AI or ML technologies, however they are out of the scope of this paper.

[2]In the context of stating lossy reconstruction with distortion level as a parameter, the concept also includes lossless case by setting the distortion parameter at zero.

[3]By utilizing broadband signaling techniques, transmission can be completed within the fading coherence time. However, it imposes severe fading frequency selectivity, resulting in inter-symbol interference (ISI). The detrimental effects due to the severe ISI caused by the fading Frequency-Selectivity can be eliminated by a proper use of Equalization, and thereby the performance with the frequency-flat static channel can be recovered, *block-by-block*, yielding Maximum Ratio Combining diversity gain on the outage probability. This indicates that the signal energy spread over the multipath components can be coherently recovered by a proper use of Equalization Techniques, resulting in the Matched Filter Bound performance [34]. Therefore, the outage probability calculated assuming block fading model is an upper bound. However, since the calculated outage curves are exact in the scenario setup assumed, it is not mentioned that the calculated outage is upper bound.

also identified for independent and correlated fading cases in the second stage.

The rest of the paper is organized as follows. Section II presents the system model and provides its mathematical formulation with the assumptions on the block fading channel models. Section III derives and analyzes the admissible RD regions with the two WZ stages considering requirements on the tolerable maximum distortion levels at Helper and Destination as parameters. Section III also introduces the DTF to connect the two stages of admissible RD regions. Section IV first calculates the system outage probability by numerically calculating the area integral, and the numerical results are then examined given the distortion requirement for independent and correlated fading at the second stage. Finally, Section V concludes the paper.

II. System Model

In this Section, the system model used in this paper is described. This paper does not focus on any specific applications, such as that shown in Fig. 1, but rather includes any system having a two-stage WZ's logical structure. Therefore, we use as much as possible mathematical expressions to express the roles of the function blocks. Since they refer to different purposes, we distinctively use *phase* and *stage* to describe, respectively, the physical operation and the successive logical structure. Accordingly we consider three phases, one sensing and two transmission phases in the one-source, one-helper, two-stage WZ communication model investigated in this paper. The first phase involves observation of the target by Source and Helper from different positions, which make the observations by Source and Helper are not exactly the same but correlated. The second and the third phases are for the communications over the wireless links. In the second phase, Source broadcasts the entropy-encoded version of the target information to Helper and to Destination. In the third phase, Helper transmits the reconstructed version of the target information, which may be distorted[4] due to the transmitted signal power restriction at Source, resulting in Source-Helper link's channel capacity being unable to support the entropy-coded target information rate.

In addition, there are two stages, the stage 1 and the stage 2, indicated by blue and red in Fig. 2, respectively. In stage 1, Helper aims to reconstruct the target information based on the observation transmitted from Source and its own observation. In stage 2, Destination then aims to reconstruct the target information based on the observation transmitted from Source and the helper information. As stated before, the system shown in Fig. 2 can be seen as two distributed multi-terminal lossy and/or lossless source coding *stages* which are successively connected.

For the performance analysis of the two-stage WZ system, we first derive the achievable RD regions with the stage 1 and the stage 2 independently. We then introduce the DTF to calculate the admissible RD region over the three transmission rates R_0, R_1, and R_2 of the system. According to the block Rayleigh fading assumption for the communication links in the stage 2, the channels stay constant over one transmitted block while varying block-by-block. We derive a theoretical expression of the outage probability, which is expressed as a two-fold area integral concerning the PDFs of the instantaneous signal-to-noise power ratio (SNR). The integral boundary conditions correspond to the RD regions with the stages 1 and 2.

[4]The distortion may occur during the wireless transmission of the entropy-coded target information, or due to the lossy compression at Source or Helper which is needed because the supported rates by the links is not large enough. However, examining the error cause is out of the scope of this paper.

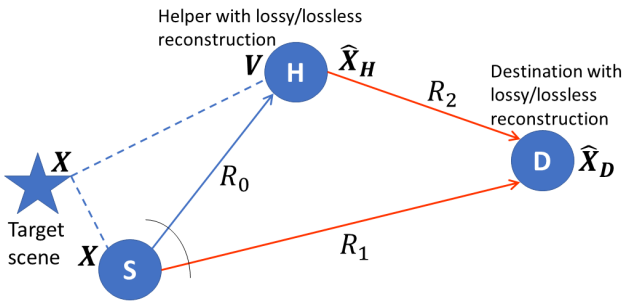

Fig. 2. One Source one Helper two-stage successive WZ simplified system model. The first stage observation (dashed lines) and communication (solid line) links are in blue, and the second stage WZ orthogonal communication links are in red.

A. Two-Stage WZ LF Relaying

Assume that for the simplicity of the analysis, the coded versions of the observed information and transmitted information are expressed by a codeword selected from a binary codebook. Extensions to the cases using the non-binary or Gaussian codebook are straightforward [38]. The first WZ stage, the stage 1, comprises target observation and Source-Helper transmission phases with the objective of reconstructing the target information for making a tentative decision at Helper. We assume that Source is close enough to the target, and hence the observation of the target is perfect. For the ease of mathematical manipulation, we consider that the discrete memoryless source X generates length-n independent and identically distributed (i.i.d.) binary sequences, $\mathbf{x} = (x(i))_{i=1}^{n}$ defined over the alphabet $\mathcal{X} = \{1, 0\}$ with i being the time index[5]. However, the rate R_0 of the Source-Helper link may not be able to support the rate for transmitting the entropy-coded target information. Hence the packet received by Helper may likely be distorted due to lossy compression at Source or errors occurring during the Source-Helper link transmission. Helper observes the target at a place different from Source; therefore, the observed information at Helper is different from, but correlated to X. The observed information V at Helper is also modeled by a discrete memoryless i.i.d. sequence $\mathbf{v} = (v(i))_{i=1}^{n}$ taken from the binary alphabet $\mathcal{V} = \{1, 0\}$ at each time index i. We assume an i.i.d bit-flipping model to express the correlation between X and V, as $V = X \oplus E$, with

[5]$\mathbf{x}$ is equivalent to the binary entropy-coded version of the target at Source under the perfect observation model.

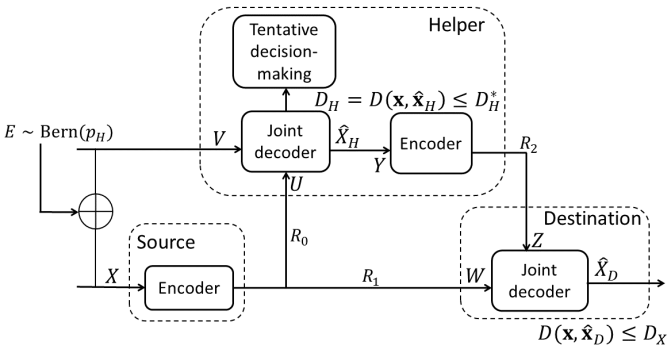

Fig. 3. Detailed block diagram of the two-stage successive WZ system.

$E \sim \text{Bern}(p_H)$ and p_H being the bit-flipping probability[6], where $p_H = 0$ and $p_H = 0.5$ are extreme cases where the correlation is one and zero, respectively. In the following, we assume that the bit-flipping probability p_H is a constant parameter because it depends only on physical conditions such as camera orientation.

The second phase in stage 1 involves packet transmission from Source to Helper[7]. The decoder at Helper uses the sequence $\mathbf{v}$ together with the sequence $\hat{\mathbf{x}}$, received via the Source-Helper link, and provides an estimate $\hat{\mathbf{x}}_H = (\hat{x}_H(i))_{i=1}^n$ of $\mathbf{x}$. With the Hamming distortion measure between $x(i)$ and $\hat{x}_H(i)$ being

$$d\left(x(i), \hat{x}_H(i)\right) = \begin{cases} 1, & \text{if } x(i) \neq \hat{x}_H(i) \\ 0, & \text{otherwise,} \end{cases} \tag{1}$$

the average distortion between the sequences $\mathbf{x}$ and $\hat{\mathbf{x}}_H$ is defined as

$$D_H = D(\mathbf{x}, \hat{\mathbf{x}}_H) = \frac{1}{n} \sum_{i=1}^{n} d(x(i), \hat{x}_H(i)). \tag{2}$$

The average distortion at Helper is an important parameter not only to evaluate the accuracy of the stage 1, but also to identify reasonable distortion allocation in both stage 1 and stage 2. We define the maximum acceptable distortion $D_H^\star \in [0, 0.5)$ specified by the tentative decision-making process at the stage 1. Eventually, $D_H^\star = 0$ corresponds to lossless requirement and $D_H^\star \neq 0$ to lossy. Obviously, the distortion D_H at Helper depends on the rate R_0 supported by the Source-Helper link and on the correlation between X and V.

The objective of the second WZ stage is to reconstruct at Destination another version $\hat{X}_D$ of the target information, while keeping the final distortion lower than the Destination's distortion requirement D_X, by utilizing the lossy and/or lossless versions of the target information transmitted via the Source-Destination and the Helper-Destination links. However, because of the fading due to the mobility of Destination, the Source-Destination link may not be able to support a rate R_1. Moreover, after the source reconstruction at the stage 1, Helper encodes and transmits the sequence $\hat{\mathbf{x}}_H$ to Destination, but the rate R_2 supported by the Helper-Destination link may not be large enough to recover the target information with the distortion requirement D_X only from $\hat{\mathbf{x}}_H$. There arises, however, a possibility that the distortion of the reconstructed target information can be made smaller than D_X by joint decoding, i.e., $D(\mathbf{x}, \hat{\mathbf{x}}_D) \leq D_X$ with $\hat{\mathbf{x}}_D$ being the joint decoder output.

Whether or not $D(\mathbf{x}, \hat{\mathbf{x}}_D) \leq D_X$ can be satisfied depends on the rate triplet (R_0, R_1, R_2), and since the two stages are connected, the criterion on the triplet requirement also depends on the distortion D_H of $\hat{\mathbf{x}}_H$ reconstructed by Helper with the help of the observation correlation knowledge at the stage 1. With a distortion requirement D_X at Destination, together with the knowledge of the bit-flipping probability p_H between X and V given, the admissible RD region $\mathcal{R}(D_X)$ of the two-stage successive WZ system involves all the rate triplets (R_0, R_1, R_2), as

$$\mathcal{R}(D_X) = \{(R_0, R_1, R_2) : (R_0, R_1, R_2) \text{ is admissible if } \lim_{n\to\infty} \mathbb{E}(D(\mathbf{x}, \hat{\mathbf{x}}_D)) \leq D_X + \epsilon, \forall \epsilon > 0\}, \tag{3}$$

for which exact expression of the region is derived in Section III.

As stated before, the system performance analysis can be decomposed into two lossy distributed coding problems where, since the stage 2 is successively connected to the stage 1, its performance is affected by the distortion D_H resulted from the stage 1. We start our investigations by analyzing the admissible RD region with the stage 1 for a given distortion requirement $D_H^\star$ at Helper. Then, the second stage analysis follows, where the distortions D_H $(\leq D_H^\star)$ and D_X at Helper and at Destination, respectively, are taken into account independently. The two stages are then connected to analyze the rate-distortion region of the two-stage successive WZ system with D_X as a parameter.

Remark: For the first stage, we used the WZ theorem which requires that $U \to X \to V$ forms a Markov chain as U represents the encoded and transmitted information of X, Therefore, U is computed only from X, and the bit flipping probability between U and X corresponds to the distortion D_H. According to the source model, X also depends on V and the bit flipping probability between X and V is defined as p_H. In the second stage, Z is the side information obtained from the encoding of Y with a bit-flipping probability equal to p, and W is the reconstructed version of the source information X and suffering from a bit-flipping distortion D_X. Finally, Y is the result of the stage 1 reconstruction at the helper, and it is correlated with X with a bit-flipping probability D_H. Hence, $Z \to Y \to X \to W$ forms a Markov chain.

B. Channel Model

Destination is assumed to be moving while Source and Helper are fixed. Hence, the Source-Destination and the Helper-Destination links suffer from fading. The complex channel gains h_1 and h_2 representing the Source-Destination

[6]This i.i.d. bit-flipping model should be able to be extended to any cardinality size of the codebook definition alphabet set. Also, the i.i.d. error assumption should be able to be replaced by an observation error model with memory. However, observation error model matching is out of the scope of this paper.

[7]It should be noted that since we assume Shannon's lossy/lossless source-channel separation theorem for the RD region and the outage derivations, we consider source coding rate only at this point of the paper.

and the Helper-Destination links' block Rayleigh fading, respectively, follow a complex Gaussian distribution $h_1, h_2 \sim \mathcal{CN}(0,1)$. The source sequence $\mathbf{x}$ is channel-encoded and modulated onto a complex symbol vector $\mathbf{x}_T$ which is transmitted to Destination. The corresponding received sequence is expressed as

$$\mathbf{w} = \sqrt{G_1} h_1 \mathbf{x}_T + \mathbf{n}_S, \tag{4}$$

where G_1 is the geometric gain [39] of the Source-Destination link, and $\mathbf{n}_S$ represents the zero-mean complex additive white Gaussian noise (AWGN) sequence. Using the same notation as in the Source-Destination link, the transmission over the Helper-Destination link is expressed as

$$\mathbf{z} = \sqrt{G_2} h_2 \mathbf{y}_T + \mathbf{n}_H, \tag{5}$$

with G_2 being the Helper-Destination link's geometric gain, $\mathbf{n}_H$ the AWGN component, and $\mathbf{y}_T$ the complex symbol sequence corresponding to the channel-encoded version of the reconstructed source information $\hat{\mathbf{x}}_H$ at Helper. The geometric gain G_1 being normalized to unity, the Helper-Destination link geometric gain can be defined as $G_2 = (\frac{d_1}{d_2})^\nu$ with d_1 and d_2 being the Source-Destination and the Helper-Destination distances, and ν is the path loss exponent. In the model of the Source-Helper link used in this paper, the cameras of Source and Helper are fixed and located at relatively high positions to have wide visions. Therefore, we assume that the Source-Helper link is dominated by the line-of-sight (LoS) component, and hence the Source-Helper link is *static*[8] by ignoring the very weak non-LoS (NLoS) components for simplicity, as in [36]. For the sake of simplicity, the effect of shadowing is also ignored for all the links.

Denote the transmitted power at Source and Helper by E_X and E_Y, respectively, and the per-dimension variance of the noise components by $N_0/2$, which is common to Source and Helper. The average SNRs on the Source-Destination and the Helper-Destination links are, respectively, expressed by $\Gamma_S = G_1 \frac{E_X}{N_0}$ and $\Gamma_H = G_2 \frac{E_Y}{N_0}$, with which the instantaneous SNRs with the two links are given by $\gamma_S = |h_1|^2 \Gamma_S$ and $\gamma_H = |h_2|^2 \Gamma_H$. Under the block Rayleigh fading assumption, the Source-Destination and the Helper-Destination instantaneous SNRs over each block follow exponential distribution with PDFs, as

$$p(\gamma_i) \quad = \quad \frac{1}{\Gamma_i} \exp(-\frac{\gamma_i}{\Gamma_i}), \quad i \in \{S, H\}. \tag{6}$$

III. Rate-Distortion System Analysis

In this Section, we present admissible RD regions for the two communication stages using the WZ theorem with the distortion requirements $D_H^\star$ and D_X at Helper and Destination, respectively, as parameters. The entropy of a random variable $X \in \mathcal{X}$ that follows a probability mass function $p(x)$ is given by

$$H(X) = -\sum_{x \in \mathcal{X}} p(x) \log p(x), \tag{7}$$

where for the particular case of the binary alphabet $\mathcal{X} = \{0, 1\}$ with $p(x = 0) = p$, we define the binary entropy function as $H(X) = H_b(p) = -p \log(p) - (1-p) \log(1-p)$.

We denote the mutual information between two random variables $X \in \mathcal{X}$ and $Y \in \mathcal{Y}$ as

$$\begin{aligned} I(X;Y) &= -\sum_{(x,y) \in \mathcal{X} \times \mathcal{Y}} p(x,y) \log \frac{p(x,y)}{p(x)p(y)} \\ &= H(X) - H(X|Y) \end{aligned} \tag{8}$$

A. Stage-by-Stage Rate-Distortion Analysis

1) Stage 1 Admissible Rate-Distortion Region: The stage 1 involves observation of the target by Source and Helper, followed by Source-to-Helper transmission. Helper aims to reconstruct the target information, which may be lossy or lossless, for making the tentative decision. Since we assume perfect target observation at Source, the system is equivalent to lossy source coding with side information for which the rate R_0 should satisfy the WZ RD function [11] which is, for general sources, given by

$$R_0 \geq I(X; U|V), \tag{9}$$

where U is an auxiliary variable representing the encoded and transmitted information for X. Since $U \rightarrow X \rightarrow V$ forms a Markov chain with respective bit flipping probabilities D_H and p_H, the mutual information in (9) can be rewritten as

$$\begin{aligned} R_0 &\geq H(U|V) - H(U|V,X) \\ &= H(U|V) - H(U|X) \\ &= H_b(D_H * p_H) - H_b(D_H), \end{aligned} \tag{10}$$

where the operator $*$ denotes the binary convolution defined as $x * y = x(1-y) + y(1-x)$.

With Helper's tolerable maximum distortion $D_H^\star$ being given as a parameter, the required Source-to-Helper link rate R_0 can be calculated as a function of the bit-flipping probability p_H. If the target observations X and V by Source and Helper are independent, then $p_H = 0.5$. In this case, the required distortion $D_H^\star$ can be satisfied only by independent decoding when $R_0 \geq 1 - H_b(D_H^\star)$, according to the binary point-to-point test channel's RD function [38]. Oppositely, if the observations by Source and Helper are correlated, the bit-flipping probability p_H decreases, resulting in that a lower Source-Helper link rate R_0 is required to satisfy $D_H^\star$. This finding agrees with the results shown in [28]. Moreover, since H_b is an increasing function when its argument value is between 0 and 0.5, it can be found from Eq. (10) that the distortion D_H of the first stage can be reduced if the observation by Helper is highly correlated with that by Source, or if Source-Helper link can support higher rate. This is useful when our objective is simply to reduce the distortion D_X at Destination, and when R_0 and p_H are the *fixed* design

[8] In practice, the second-order statistics representing the memory structure of the channel variation is not fully identified, and up to the authors' best knowledge, only a few derived expressions are known, e.g., [40], but they are highly propagation model-dependent. In this sense, how we can best exploit the advantage of memory-channel over memory-less channel, both block-by-block, is left as an open question.

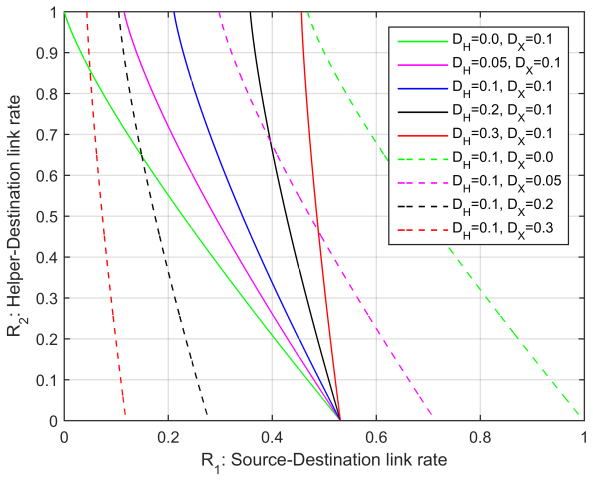

Fig. 4. Admissible RD region for the stage 2 with different distortions D_H at Helper, and for different distortion requirements D_X at Destination.

parameters[9]. Given the first stage distortion D_H, the rates R_1 and R_2 in the second stage can be identified, which determines the distortion D_X at Destination.

2) Stage 2 Admissible Rate-Distortion Region: The stage 2 is based on the two orthogonal communication steps over the Source-Destination and the Helper-Destination links with their rates R_1 and R_2, respectively. Obviously, the logical structure of the system is equivalent to single-helper assisted distributed lossy coding where the reconstructed source information by Helper, represented by Y, has a distortion D_H measured by the Hamming distortion from the source information X. Since X and Y are correlated, this stage is also equivalent to lossy distributed source coding of which WZ admissible RD region [11] is specified by

$$R_1 \geq I(X;W|Z) \tag{11}$$
$$R_2 \geq I(Y;Z) \tag{12}$$

with auxiliary variables W and Z representing, respectively, the reconstructions of X and Y, encoded and transmitted from Source and Helper, at Destination as depicted in Fig. 3.

Since $Z \rightarrow Y \rightarrow X \rightarrow W$ forms a Markov chain parameterized by the bit flipping probability and Hamming distortions, p, D_H, and D_X, respectively, Eq. (11) can be expressed as

$$\begin{aligned} R_1 &\geq H(W|Z) - H(W|Z,X) \\ &= H(W|Z) - H(W|X) \\ &= H_b(p * D_H * D_X) - H_b(D_X). \end{aligned} \tag{13}$$

With the assumption of the uniformly distributed binary source X with the i.i.d. random bit flipping error model between X and Y, $H(X) = H(Y) = 1$. Hence,

$$R_2 \geq H(Y) - H(Y|Z) = 1 - H_b(p). \tag{14}$$

Besides the final distortion D_X, as shown in (13) and (14), the admissible RD region of the second stage depends on D_H, and the Helper-Destination link's bit flipping probability p. Fig. 4 shows the admissible RD region of the stage 2 with D_H and D_X as parameters where the solid and dashed curves are for $D_X = 0.1$ and $D_H = 0.1$, respectively. The value of p is determined from Eq. (14), by $p = H_b^{-1}(1-R_2)$ where $H_b^{-1}(.)$ is the inverse of the binary entropy function [14]. Fig. 4 shows that, when R_1 is large enough for independent decoding, the side information provided by Helper in R_2 becomes redundant. This case follows the test channel model [38] of point-to-point communication corresponding to the RD function $R_1 \geq 1 - H_b(D_X)$, and is independent of the distortion D_H. Note that the case $R_1 = 1$ corresponds to lossless recovery $D_X = 0$. However, when R_1 is not large enough to guarantee the distortion requirement at Destination, R_2 should be increased to compensate the decreased R_1. In this case, the value of R_2 depends on the stage 1 distortion D_H at Helper. For example, if the Source-to-Helper communication in the first stage is lossless, e.g., $D_H = 0$, the admissible RD region is equivalent to that obtained in [28] for lossy-forward relaying where the bit-flipping probability due to the errors occurring in the Source-Helper link is set at 0. It is also clear that the admissible RD region becomes larger when the distortion D_H at Helper becomes smaller. Even with $R_2 = 1$, $R_1 = H_b(D_H * D_X) - H_b(D_X) > 0$ is required if $D_H \neq 0$ due supposedly to the *insufficient* rate R_0 supported by the Source-Helper link and/or *low* correlation between the two observations at the stage 1. Another interesting finding is, as demonstrated by the dashed lines, that the admissible rate-distortion region becomes remarkably larger when Destination can accept large distortion D_X. It is also worth noticing that the slopes of the admissible RD region boundaries are the same when the values of D_X and D_H are interchanged, i.e., the two curves with the same color are parallel each other, and the slope is $1/(H_b(D_H * D_X) - 1)$.

The stage-by-stage admissible RD region analysis presented above is useful for applications where a tentative decision's tolerance criterion $D_H^\star$ is required at Helper. In this case, depending on the correlation between the observations by Source and Helper, the rate constraint is identified for the Source-Helper link to achieve the required distortion at the stage 1. Given the distortion requirement $D_H \leq D_H^\star$ of the stage 1, the admissible RD region is then fully identified by Eqs. (13) and (14) for the stage 2, which satisfies the distortion requirement D_X at Destination. It is clear that the two stages can be studied separately for such applications.

B. Distortion Transfer Function for Two-Stage WZ System Analysis

This sub-section derives the global system's RD region, by connecting the two WZ stages, with the bit-flipping probability p_H of the observation by Helper and the final distortion D_X as parameters. We do not consider the constraint imposed on the stage 1 distortion D_H at Helper as long as D_X is satisfied, for which the region of the rate triplet (R_0, R_1, R_2) has to be plotted. To connect the two stages, the distortion D_H at Helper is a crucial parameter since it depends on the bit flipping probability p_H and the rate R_0 in the stage 1,

[9]It should be noticed that this finding is only the case that the transmission part of the stage 1 is over the static Source-Helper link

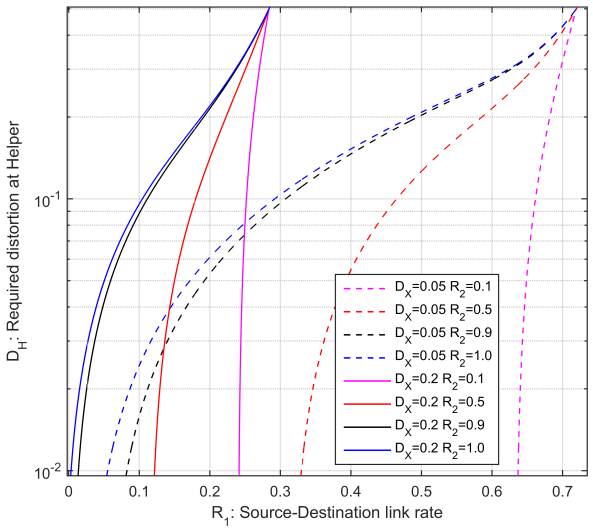

Fig. 5. The required Helper distortion $D_H^\star$ as a function of the Source-Destination link rate R_1 for different Helper-Destination link rates R_2 and destination distortion requirements D_X.

and significantly impacts the admissible RD region of the stage 2. To mathematically analyze the impact of D_H on the admissible RD region of the stage 2, we introduce a function for computing an upper bound of binary convolutions.

Proposition. *For any values* $x, t \in [0, 0.5]$ *and* $y \in [0, 0.5)$, *if* $x * y = x(1-y) + y(1-x) \leq t$, *then*

$$x \leq \Lambda(y,t) \triangleq \frac{1}{2}\left(1 - \frac{2t-1}{2y-1}\right). \tag{15}$$

The proof is trivial using the binary convolution definition.

As shown in Appendix A, when t is fixed, $\Lambda(y,t)$ is an inversely decreasing function of y, and it takes its maxima $\Lambda(y,t)_{max} = t$ with $y = 0$. Hence, if the convolution $x * y$ is upper-bounded by t, then x is upper-bounded by $\Lambda(y,t) \leq t$, which imposes a constraint on x, depending on the value of y.

Lemma. *For any probabilities* $x, t \in [0, 0.5]$ *and* $y, z \in [0, 0.5)$, *if* $x * y * z \leq t$, *then*

$$x \leq \Lambda(y, \Lambda(z,t)). \tag{16}$$

The proof is a trivial extension of Proposition.

For the first WZ stage, Eq. (10) can be rewritten using the Λ-function to more clearly identify the impact of p_H, the observation correlation between Source and Helper, given the rate R_0 supported by the Source-Helper link and the required distortion $D_H = D_H^\star$ at Helper. Given that H_b^{-1} is an increasing function, using Proposition, we have

$$p_H \leq \Lambda(D_H^\star, H_b^{-1}(R_0 + H_b(D_H^\star))). \tag{17}$$

This equation shows that the Λ-function transfers the constraint on the stage 1 distortion $D_H^\star$ at Helper, to a constraint on the bit-flipping probability p_H of the observation by Helper which is equivalent to the distortion on the side information V for Helper with respect to X. In the case the distortion requirement $D_H^\star$ is satisfied only by the Source-Helper rate being $R_0 \geq 1 - H_b(D_H^\star)$, with which $\Lambda(y, 0.5) = 0.5$ indicating no side information is required. When a larger distortion $D_H^\star$ at Helper can be tolerated, or when the Source-Helper link's supported rate R_0 increases, the requirement for the correlation between observations by Source and Helper can be relaxed, and hence relatively larger p_H can be tolerated.

Similarly, we can use the Λ-function to transfer the stage 2 distortion requirement D_X at Destination, to the stage 1 distortion requirement on D_H at Helper. Given that H_b^{-1} is an increasing function, by utilizing Lemma, we can identify the distortion $D_H^\star$ at Helper required to be satisfied after the first stage based on parameters D_X and R_1, as

$$D_H^\star \leq \Lambda\left(p, \Lambda(D_X, H_b^{-1}(R_1 + H_b(D_X)))\right). \tag{18}$$

When the rate R_2 supported by Helper-Destination link is large enough to guarantee error free transmission with $p = 0$, then by setting $\Lambda(0,t) = t$, the upper bound on $D_H^\star$ reduces to $\Lambda(D_X, H_b^{-1}(R_1 + H_b(D_X))$ defined as D_{SI}. This is analogous to the stage 1 constraint expressed in (17), and provides the required distortion of the side information for Destination. However, when the rate R_2 supported by the Helper-Destination decreases, the error probability p increases, and since Λ is a decreasing function of its first argument, the required distortion $D_H^\star$ at Helper has to be decreased. We recall that the function $\Lambda(y,t)$ is only defined for $y \leq t$. Then, (18) turns into a condition $p \leq D_{SI}$. If this condition is not satisfied, it is impossible to achieve the distortion D_X at Destination, even with zero distortion at Helper, and as a result the outage event happens. This issue will be further discussed in Section IV.

The recursive structure shown in (18) corresponds to the cooperative communication network topology, which provides us with significant flexibility when analyzing the rate region of the network represented by lossy distributed coding systems. As the Λ-function identifies the distortion level $D_H^\star$ at Helper required to satisfy the final distortion D_X at Destination, it is called DTF in the rest of the paper.

Fig. 5 represents the distortion $D_H^\star$ required for the stage 1 versus R_1 supported by the Source-Destination link with R_2 and D_X as parameters. It is found that when the rate R_1 supported by the Source-Destination link is larger than $1 - H_b(D_X)$, the Helper has no distortion requirement, i.e., $D_H^\star = 0.5$. This corresponds to the case where the distortion requirement at Destination can be satisfied by the rate supported by the point-to-point Source-Destination link independently of p and D_H. However, when R_1 decreases to lower than $1 - H_b(D_X)$, the side information provided by the Helper-Destination link is needed, and the required distortion $D_H^\star$ at Helper decreases very quickly. When $R_2 = 1$ (blue curves), the Helper-Destination link is error free $p = 0$, and the required distortion $D_H^\star$ correspond to the required side information distortion D_{SI}. When the Helper-Destination link's supported rate R_2 decreases, this results in higher error probabilities p, and lower distortion is required at Helper. Moreover, in this case, even with a lossless communication at the stage 1 yielding $D_H = 0$, a condition on $R_1 \geq H_b(D_X * p) - H_b(D_X)$ is required to support $p \leq D_{SI}$.

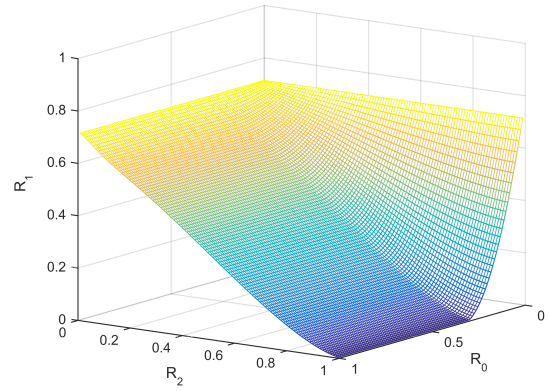

(a) $D_X = 0.05$, $1 - H_b(D_X) = 0.71$, $p_H = 0.05$, $H_b(p_H) = 0.28$

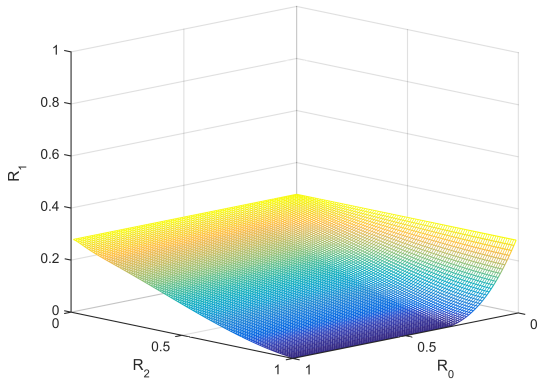

(b) $D_X = 0.2$, $1 - H_b(D_X) = 0.27$, $p_H = 0.05$, $H_b(p_H) = 0.28$

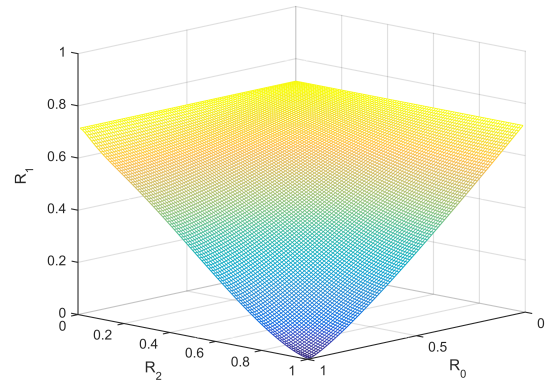

(c) $D_X = 0.05$, $1 - H_b(D_X) = 0.71$, $p_H = 0.4$, $H_b(p_H) = 0.97$

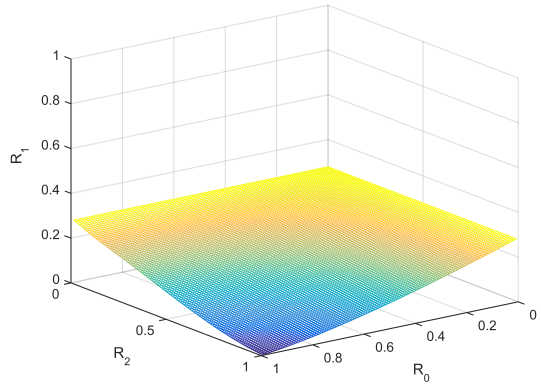

(d) $D_X = 0.2$, $1 - H_b(D_X) = 0.27$, $p_H = 0.4$, $H_b(p_H) = 0.97$

Fig. 6. The admissible RD region for the two-stage successive WZ system with lossy/lossless reconstruction at Helper for different distortions requirements D_X at Destination, and Helper to Source observations correlation.

In block fading environments, the supported rates R_1 and R_2 vary due to the instantaneous SNR variations, block-by-block. An indicative insight for the outage evaluation in fading environments which will be investigated in Section IV is that when, for example, large distortion level D_H at the stage 1 can be tolerated to make a tentative decision at Helper, the requirement on the rates R_1 and R_2 also becomes large to satisfy the distortion requirement D_X to make the final decision at Destination; the requirement is not satisfied with a certain outage probability, because the stage 1 is by observations followed by transmission over static channel, while the stage 2 is via fading channel.

C. Two-Stage Successive WZ System 3D Rate-Distortion Analysis

To have insightful observation toward a deeper understanding of the influence of each parameter on the two-stage WZ system's RD region defined in Eq. (3), this subsection provides three-dimensional (3D) figures to visualize the rate triplet surface (R_0, R_1, R_2). The result is shown in Fig. 6 with respect to the parameter correlation p_H of the observations between Source and Helper, and the distortion D_X at Destination. Figs. (6a)–(6d) illustrate the admissible rate-distortion surfaces for the four combinations of the bit-flipping probability $p_H \in \{0.05, 0.4\}$ and tolerable distortion $D_X \in \{0.05, 0.2\}$ at Destination. First of all, it is clearly found that arbitrary R_0 and R_2 values are admissible as long as the rate R_1 supported by the Source-Destination link is larger than $1 - H_b(D_X)$, which corresponds to the rate for lossy point-to-point communication over the Source-Destination link alone. It is also found by comparison between Figs. (6a) and (6b) as well as between Figs. (6c) and (6d) that the two-stage WZ system's admissible RD region occupies greater volume as larger distortion is allowed at Destination. Moreover, for a given distortion requirement D_X, the admissible RD region also expands when the correlation between Source and Helper observations increases. Figs. (6a) and (6b) show the admissible region for a highly correlated case $p_H = 0.05$. It is found from those figures that when $R_0 \geq H_b(p_H)$, the admissible RD region for the rate pair R_1 and R_2 remains the same. This comes from the fact that this setup corresponds to a lossless communication at the stage 1 yielding $D_H = 0$. However,

when $R_0 < H_b(p_H)$, the corresponding non-zero distortion at Helper needs to be compensated by increasing the rates R_1 and R_2. For a given D_X, as shown in Figs. (6c) and (6d), when the observation by Helper is not highly correlated with the one by Source, $H_b(p_H)$ approaches one, and thereby higher rates, R_1 and R_2 are required on the stage 2, resulting in reduced area of the admissible rates region of R_1 and R_2.

IV. Outage Probability Analysis

Based on the admissible RD regions investigated in Section III, we can derive the outage probabilities for the two-stage successive WZ system under the system and the fading variation models given in Section II. We assume that the Source-Destination and the Helper-Destination distances are equal, which corresponds to equal geometric gains $G_1 = G_2 = 1$. Without the loss of generality, we assume normalized spectrum efficiencies $R_c^S = R_c^H = \frac{1}{2}$ for the communications over the Source-Destination and the Helper-Destination links, which corresponds to the case, for example, where a half-rate channel code with binary phase shift keying (BPSK) modulation is used. Under such assumptions, the average SNRs on the Source-Destination and the Helper-Destination links are identical, i.e., $\Gamma_1 = \Gamma_2$. Since the parameters related to the stage 1 are all *static*, we investigate the impact of the distortions D_H and D_X at Helper and Destination, respectively, on the system performance.

A. Outage Probability Derivation

An outage event occurs when the rates triplet (R_0, R_1, R_2) falls outside the admissible RD region defined in Eq. (3) for a distortion requirement D_X at Destination. As depicted in Fig. 1, the stage 1 parameters including the bit-flipping probability p_H and the Source-Helper link rate R_0 are fixed. Hence, it is reasonable that the distortion D_H at Helper is also fixed when calculating the outage probability. On the other hand, Destination is assumed to be moving, indicating that the Source-Destination and the Helper-Destination links are suffering from fading variations, and thereby their supporting rates R_1 and R_2 also change block-by-block. Correlated Rayleigh fading between the Source-Destination and the Helper-Destination links is assumed in this paper, with which statistically independent fading is a special case. Note that fading correlation is different from observation correlation. For the lossless case, impact analyses of the statistical properties of fading variations on the outage probability and the equivalent diversity order with Lossy Forward relaying are provided in [19].

Given the first WZ stage distortion D_H at Helper, an outage happens when either the rate R_1 or R_2 does not, or both do not satisfy the rate-distortion region specified by the distortion requirement D_X at Destination. Therefore, the outage probability with the two-stage successive WZ system can be expressed by twofold (area) integrals with respect to the PDF of the instantaneous SNRs of the Source-Destination and the Helper-Destination links.

Given the distortions pair (D_H, D_X), the inadmissible RD region of the stage 2 can be identified, as shown in Fig. 4. For the ease of the integral calculation, it should be noticed that the region can be split into two disjoint sub-regions, Case 1 and Case 2. The former corresponding to that for any possible values of R_2, the Source-Destination link rate $R_1 \leq H_b(D_H * D_X) - H_b(D_X)$ is not large enough to compensate the distortion D_H at Helper in order to satisfy the requirement D_X at Destination. The latter (Case 2) corresponds to the case where the distortion $p \neq 0$ caused by the rate loss on $R_2 < 1$ is not recovered by the Source-Destination link rate $R_1 \leq H_b(p * D_H * D_X) - H_b(D_X)$. The two cases are denoted C_1 and C_2, and can be written as:

$$\begin{aligned} C_1 &\triangleq \{0 \leq R_1 \leq H_b(D_H * D_X) - H_b(D_X), 0 \leq R_2\} \\ C_2 &\triangleq \{H_b(D_H * D_X) - H_b(D_X) \leq R_1 \\ &\leq H_b(p * D_H * D_X) - H_b(D_X), 0 \leq R_2 \leq 1\} \end{aligned}$$

The outage probability P_{out} can then be computed by taking the average over all the transmission rate pairs (R_1, R_2) that fall inside the rate region specified by the sets C_1 and C_2. Since C_1 and C_2 are disjoint, P_{out} can be written as:

$$\begin{aligned} P_{out} &= \Pr\{(R_1, R_2) \in C_1\} + \Pr\{(R_1, R_2) \in C_2\} \\ &= P_{out}^{C_1} + P_{out}^{C_2} \end{aligned} \tag{19}$$

Since the communication part of the stage 2 is orthogonal and is point-to-point over both the Source-Destination and the Helper-Destination links, we can use the Shannon's lossy source-channel separation theorem [33]. Hence, R_1 and R_2, required to achieve the distortion D_X at Destination as shown in Eqs. (13)–(14), can further be replaced by the channel capacities with the Source-Destination and the Helper-Destination links, as

$$R_1 \leq \Phi_S(\gamma_S) \triangleq C(\gamma_S)/R_c^S, \tag{20}$$

$$R_2 \leq \Phi_H(\gamma_H) \triangleq C(\gamma_H)/R_c^H, \tag{21}$$

where R_c^S and R_c^H represent the normalized spectrum efficiencies including the channel coding rate and the modulation multiplicity with $C(.)$ being the Shannon capacity function with Gaussian codebooks[10]. Moreover, γ_S and γ_H have been defined in (6). When two dimensional signaling is used, the Shannon capacity with the instantaneous SNR γ is expressed as $C(\gamma) = \log(1 + \gamma)$. Therefore, if the rate pair (R_1, R_2) provided by $(\Phi_S(\gamma_S), \Phi_H(\gamma_H))$ falls inside the inadmissible rate-distortion region C_1 or C_2, an outage occurs. The instantaneous SNRs γ_S and γ_H can be computed as functions of the rates R_1 and R_2, respectively, by using the inverse of functions of Φ_S and Φ_H, as $\gamma_S = \Phi_S^{-1}(R_1) = 2^{R_1 \cdot R_c^S} - 1$ and $\gamma_H = \Phi_H^{-1}(R_2) = 2^{R_2 \cdot R_c^H} - 1$. Obviously, $\Phi_S^{-1}(0) = \Phi_H^{-1}(0) = 0$. As noticed before, the RD analysis for the successive two-stage WZ system can also be used in the lossless cases by setting $D_X = 0$.

Given the distortion D_H at Helper in the stage 1 and the required distortion D_X at Destination, the outage probability $P_{out}^{C_1} = \Pr\{(R_1, R_2) \in C_1\}$ due to Case 1 can be calculated using the joint PDF of the instantaneous SNRs $p(\gamma_S, \gamma_H)$ as

$$P_{out}^{C_1} = \Pr\{0 \leq R_1 \leq L_S, 0 \leq R_2\}$$

[10]Based on the source-channel separation theorem, we assume binary source coding using binary codewords, followed by capacity-achieving channel using Gaussian codebooks.

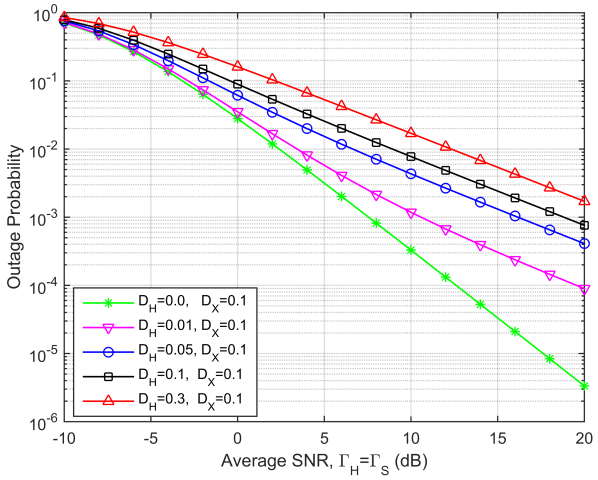

Fig. 7. Outage probability of the two-stage successive WZ system for different distortions D_H at Helper and a fixed distortion $D_X = 0.1$ at Destination.

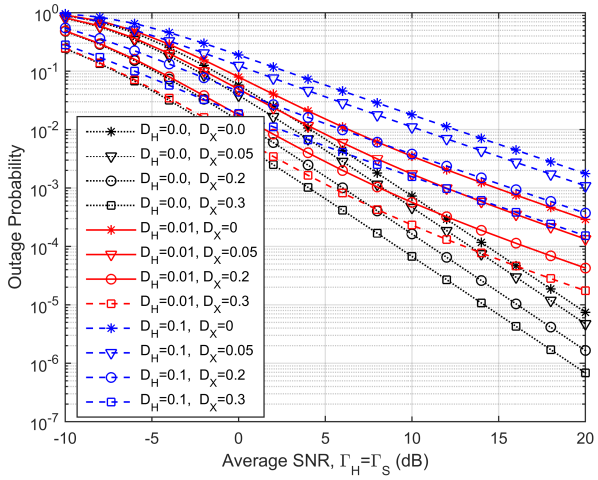

Fig. 8. Outage probability of the two-stage successive WZ system for different distortions D_X at Destination and fixed distortions $D_H = 0$, $D_H = 0.01$ and $D_H = 0.1$ at Helper.

$$
\begin{aligned}
&= \Pr\{0 \le \Phi_S(\gamma_S) \le L_S, 0 \le \Phi_H(\gamma_H)\} \\
&= \Pr\{\Phi_S^{-1}(0) \le \gamma_S \le \Phi_S^{-1}(L_S), \Phi_H^{-1}(0) \le \gamma_H\} \\
&= \int_{\Phi_H^{-1}(0)}^{+\infty} \int_{\Phi_S^{-1}(0)}^{\Phi_S^{-1}(L_S)} p(\gamma_S, \gamma_H)\, d\gamma_S\, d\gamma_H, \qquad (22)
\end{aligned}
$$

where $L_S = H_b(D_H * D_X) - H_b(D_X)$.

Case 2 includes $R_2 = \Phi_H(\gamma_H) < 1$, which results in the bit flipping probability $p \neq 0$, calculated using the Helper-Destination link's instantaneous SNR γ_H, as $p = H_b^{-1}(1 - \Phi_H(\gamma_H))$. Hence, with $H_S(\gamma_H) = H_b(H_b^{-1}(1 - \Phi_H(\gamma_H)) * D_H * D_X) - H_b(D_X)$, the outage probability $\Pr\{(R_1, R_2) \in C_2\}$ due to Case 2 is obtained by

$$
\begin{aligned}
P_{out}^{C_2} &= \Pr\{L_S \le R_1 \le H_S(\gamma_H), 0 \le R_2 \le 1\} \\
&= \Pr\{L_S \le \Phi_S(\gamma_S) \le H_S(\gamma_H), 0 \le \Phi_H(\gamma_H) \le 1\} \\
&= \Pr\{\Phi_S^{-1}(L_S) \le \gamma_S \le \Phi_S^{-1}(H_S(\gamma_H)), \\
&\quad \Phi_H^{-1}(0) \le \gamma_H \le \Phi_H^{-1}(1)\} \\
&= \int_{\Phi_H^{-1}(0)}^{\Phi_H^{-1}(1)} \int_{\Phi_S^{-1}(L_S)}^{\Phi_S^{-1}(H_S(\gamma_H))} p(\gamma_S, \gamma_H)\, d\gamma_S\, d\gamma_H \qquad (23)
\end{aligned}
$$

B. Outage Analysis in Independent Fading

Under the assumption of independent fading variations on the Source-Destination and the Helper-Destination links, by substituting Eq. (6) into Eqs. (22) and (23), the outage probabilities corresponding to Case 1 and Case 2 can be expressed by (24) and (25), respectively, where $P_{out}^{C_1}$ is a closed-form result, and $P_{out}^{C_2}$ is only a one-fold integral.

Even though we can use the simple yet accurate approximation of the inverse entropy function given by [14], still deriving explicit expression of the integrals given by Eq. (25) is not easy[11]. Hence, we use a numerical method to evaluate the integrals.

The numerical result of the outage probability for the two-stage successive WZ system is presented in Fig. 7, where the required tolerable distortion at the destination is set to $D_X = 0.1$, and the distortion D_H at Helper varies from 0.0 to 0.3. We can clearly observe from the decay of the green curve corresponding to a lossless stage 1 ($D_H = 0$) that second-order diversity can be achieved over the entire value range of the average SNR. However, when the distortion D_H at Helper increases, the decay in outage curves corresponds to second-order diversity only for low average SNR. However, the decay asymptotically merges into the first-order diversity when the average SNR value increases. It is found that the value range during which the second-order diversity can be achieved is smaller as the distortion D_H at Helper is larger. This result is consistent with the outage curves shown in [42] for a LF relaying applied to lossless communications. The result is also consistent with the analytical results presented in Fig. 5 where we demonstrated using the DTF that the required distortion D_H at Helper becomes smaller rapidly as the rates R_1 and R_2 supported by, respectively, the Source-Destination and the Helper-Destination links decrease. The asymptotic behavior of the diversity order according to the increase in average SNRs is proven in Appendix B for both lossless and lossy cases.

We then focus on the impact of the required distortion D_X at Destination on the system outage probability. Fig. 8 depicts the outage probability as a function of the average SNR of the Source-Destination and the Helper-Destination links for $D_X \in \{0, 0.05, 0.2, 0.3\}$ where black, red, and blue curves correspond to $D_H = 0$, $D_H = 0.01$ and $D_H = 0.1$,

[11]The H-Transform [41] functions including the Meijer-G and Fox-H functions are useful tools for analyzing and modeling the properties of the variation of the connected channels. However, the decoding and re-encoding processes at the LF helper break the connected channel variation occurring on the concatenated S-H-D link into S-H and H-D independent variations. Hence, with this setup, we can best utilize Shannon's separation theorem independently, link by link.

$$P_{out}^{C_1} = \frac{1}{\Gamma_S\Gamma_H}\int_{\Phi_H^{-1}(0)}^{+\infty}\int_{\Phi_S^{-1}(0)}^{\Phi_S^{-1}(L_S)} \exp(-\frac{\gamma_S}{\Gamma_S})\ \exp(-\frac{\gamma_H}{\Gamma_H})\ d\gamma_S\ d\gamma_H = 1-\exp\left(\frac{-\Phi_S^{-1}(L_S)}{\Gamma_S}\right) \quad (24)$$

$$\begin{aligned} P_{out}^{C_2} &= \frac{1}{\Gamma_S\Gamma_H}\int_{\Phi_H^{-1}(0)}^{\Phi_H^{-1}(1)}\int_{\Phi_S^{-1}(L_S)}^{\Phi_S^{-1}(H_S(\gamma_H))} \exp(-\frac{\gamma_S}{\Gamma_S})\ \exp(-\frac{\gamma_H}{\Gamma_H})\ d\gamma_S\ d\gamma_H \\ &= \frac{1}{\Gamma_H}\int_{\Phi_H^{-1}(0)}^{\Phi_H^{-1}(1)} \exp(-\frac{\gamma_H}{\Gamma_H})\left[\exp\left(-\frac{\Phi_S^{-1}(L_S)}{\Gamma_S}\right)-\exp\left(-\frac{\Phi_S^{-1}(H_S(\gamma_H))}{\Gamma_S}\right)\right]d\gamma_H \end{aligned} \quad (25)$$

respectively. It can be clearly observed that when larger distortion is tolerated at Destination, the outage probability curves have the same decay, i.e., the curves with the same D_H values indicated by the same color are parallel. In fact, the required distortion D_X at Destination has no impact on the diversity order.

As shown in Fig. 4, the smaller the value of D_X, the sharper the slope of the admissible rate region of the stage 2. However, it is found from Fig. 8 that this admissible RD slope change has no impact on the tendency of the outage probabilities diversity order. This is because when D_X decreases, the outage probability $P_{out}^{C_1}$ dominates the system outage probability, and the contribution of Case C_2 becomes smaller. This observation justifies that the tendency of the diversity order remains the same. This asymptotic tendency is also supported mathematically in Appendix B.

C. Outage Analysis in Correlated Fading

In practice, the fading variations happening on different links are often correlated because of insufficient spatial or temporal separation between the communicating nodes. We use $\rho = \langle h_1 h_2^* \rangle$ to denote the correlation of the channel gains h_1 and h_2 occurring at the Source-Destination and the Helper-Destination links[12], respectively, where $|\rho| = 0$ corresponds to independent fading, for which outage probability has been investigated in sub-section IV-B. When $|\rho| \neq 0$, the joint PDF of the instantaneous SNRs γ_S and γ_H is given by [19]

$$\begin{aligned} p(\gamma_S,\gamma_H) = &\frac{1}{\Gamma_S\Gamma_H(1-|\rho|^2)}\exp\left(-\frac{1}{1-|\rho|^2}(\frac{\gamma_S}{\Gamma_S}+\frac{\gamma_H}{\Gamma_H})\right) \\ &\times I_0\left(\frac{2|\rho|}{1-|\rho|^2}\sqrt{\frac{\gamma_S\gamma_H}{\Gamma_S\Gamma_H}}\right), \end{aligned}$$

with $I_0(x)$ being the zero-th order modified Bessel's function of the first kind. It can be expressed using its series expansion [43] as

$$I_0(x) = \sum_{m=0}^{+\infty}\frac{1}{(m!)^2}\left(\frac{x}{2}\right)^{2m}. \quad (26)$$

Then, the outage probabilities corresponding to Case 1 and Case 2 can be, respectively, approximated by taking the first M terms, as in Eqs. (27) and (28) with

$$a = \frac{1}{1-|\rho|^2}, \quad (29)$$

[12]We characterize mathematically the channel correlation by the parameter ρ, which allows us to analyze the outage probability without considering any practical propagation models.

$$A_m = \frac{1}{\Gamma_S\Gamma_H(m!)^2}\frac{|\rho|^{2m}}{(1-|\rho|^2)^{2m+1}}. \quad (30)$$

Remark: It is well known that the Taylor series expansion of the Bessel function is quite accurate and has been widely used [19]. In fact, we utilized in this paper, a term-by-term convergence test where the value difference between the two consecutive indexes in the summation is checked and if the difference is found to be less than a specified small value, the calculation for the summation is stopped. Appendix C provides the stability proof and the justification of the numerical calculations by using the Taylor Series expansion of the modified Bessel Function of the first kind. Analyzing the impact of inaccuracy of the series expansion at very detailed level is left as future research.

Based on the outage probability expression, the numerical method used in the independent fading case can also be used to evaluate the outage probability where the summations are calculated for increasing m until convergence. As assumed in the independent case, the parameters from the stage 1 are fixed and the Source-Destination and the Helper-Destination links experience identical average SNRs. The results are presented in Fig. 9 where the impact of the fading correlation ρ is analyzed for different distortion requirements at Helper and Destination. Fig. 9 (a) presents the results for the case where the stage 1 is assumed to be lossless, providing $D_H = 0$. Clearly, for a given distortion requirement D_X at Destination, the larger the fading correlation, the higher the outage probability. However, when the average SNR is large, second-order diversity can be achieved for $D_H = 0$, regardless of D_X and ρ values. As in the independent fading case, larger distortion D_X at Destination can be tolerated, smaller outage probability can be achieved. The curves are all parallel-shifted, and the shift depends on the considered parameters. The curves in Fig. 9 (b) show that when $D_H \neq 0$ at Helper, the asymptotic behavior of the outage probability changes to the first-order diversity. However, depending on the value of D_H and on the links correlation $|\rho|$, the second-order diversity can be achieved at medium values range of the average SNR. The average SNR on which we observe a second-to-first diversity order change is higher when D_H and $|\rho|$ are smaller. We finally conclude that when the Helper-Destination and the Source-Destination links are more highly correlated, the outage probability becomes larger. However, the fading correlation has no impact on the diversity order at high average SNRs value range, as we observed in the case of the independent Helper-Destination and

$$P_{out}^{C_1} \approx \sum_{m=0}^{M} A_m \int_{\Phi_H^{-1}(0)}^{+\infty} \int_{\Phi_S^{-1}(L_S)}^{\Phi_S^{-1}(L_S)} \left(\frac{\gamma_S \gamma_H}{\Gamma_S \Gamma_H}\right)^m \exp\left(-a\frac{\gamma_S}{\Gamma_S}\right) \exp\left(-a\frac{\gamma_H}{\Gamma_H}\right) \, d\gamma_S \, d\gamma_H \tag{27}$$

$$P_{out}^{C_2} \approx \sum_{m=0}^{M} A_m \int_{\Phi_H^{-1}(0)}^{\Phi_H^{-1}(1)} \int_{\Phi_S^{-1}(L_S)}^{\Phi_S^{-1}(H_S(\gamma_H))} \left(\frac{\gamma_S \gamma_H}{\Gamma_S \Gamma_H}\right)^m \exp\left(-a\frac{\gamma_S}{\Gamma_S}\right) \exp\left(-a\frac{\gamma_H}{\Gamma_H}\right) \, d\gamma_S \, d\gamma_H \tag{28}$$

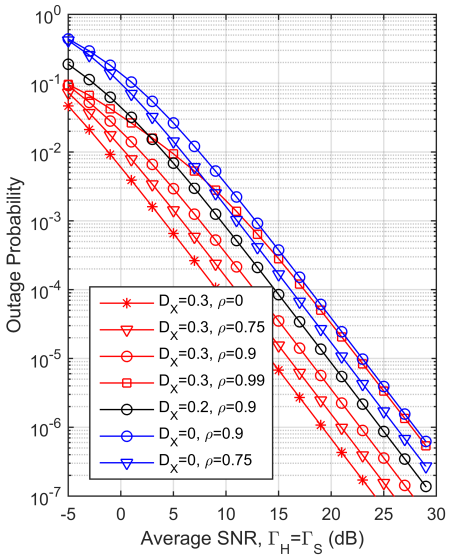

(a) Lossless stage 1: $D_H = 0$

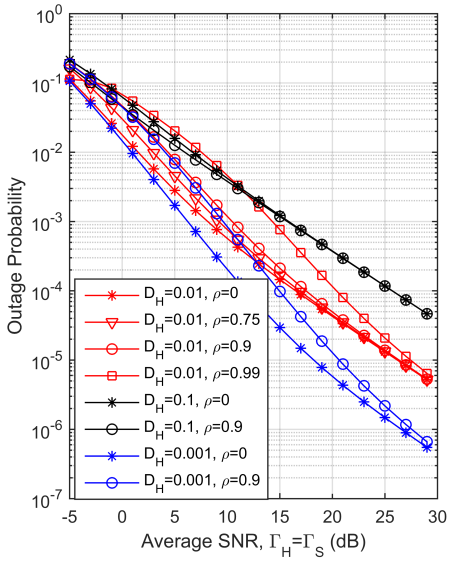

(b) Fixed distortion requirement at Destination $D_X = 0.2$

Fig. 9. Outage probability of the two-stage successive WZ system for different fading correlation coefficient ρ with different distortions D_X at Destination and D_H at Helper.

Source-Destination links scenario. This asymptotic behavior is mathematically proven in Appendix D.

V. Conclusions

In this paper, the outage probabilities of two-stage successive Wyner-Ziv relaying have been evaluated, where it is assumed that neither Source-Helper nor Source-Destination communications have to be lossless. The system is divided into two successive stages for which the admissible rate-distortion (RD) regions have been investigated. Moreover, a distortion transfer function (DTF) has been proposed as a mathematical tool for analyzing how the distortions at each stage affects to (or is affected by) its connected stages. A three dimensional plot of the whole system's admissible RD region has then been calculated using the DTF. It is shown that the admissible RD region becomes larger remarkably when the tolerable distortion at Destination is higher. Furthermore, when the observations by Source and Helper are highly correlated, the required Source-Helper link rate can be reduced which makes the whole system's admissible rate region even larger. Then, based on Shannon's lossy source-channel separation theorem, this paper has calculated the two-stage WZ system's outage probabilities under the assumption of static links with the stage 1 and block Rayleigh fading links with the stage 2. Numerical results for the outage probabilities have been presented with different distortion levels at Helper and Destination parameters in independent and correlated fading variations. The results demonstrate that the impact of the distortion tolerated by Helper appears in the form of diversity order in the outage probability curves; a second-order diversity can be achieved only if the reconstruction at Helper is perfect, and the diversity order plateaus at the first order asymptotically by increasing averages SNR if the reconstruction is imperfect. Moreover, when the end-to-end required system distortion is larger, the outage probability decreases while keeping the same diversity order. This asymptotic tendency of the outage probability remains the same for independent and correlated fading. We can finally conclude that with very smart decision-making machines that can tolerate larger distortions, the total power consumption can be reduced while keeping a certain level of the outage probability, required for critical services with fading link qualities such as in C-V2X.

Appendix A
Analysis of the Function $\Lambda(y,t)$

The Distortion Transfer Function $\Lambda(y,t)$ defined in Eq. (15) has two partial derivatives

$$\frac{\partial \Lambda(y,t)}{\partial y} = \frac{2t-1}{(2y-1)^2} \leq 0, \tag{31}$$

and

$$\frac{\partial \Lambda(y,t)}{\partial t} = \frac{-1}{(2y-1)} > 0. \tag{32}$$

Hence, $\Lambda(y,t)$ is a monotonically decreasing function of its first argument y. For a given $t \in [0, 0.5]$, $\Lambda(y,t)$ reaches its maximum at $y = 0$, with $\Lambda(y = 0, t) = t$, and its minimum at $y = t$ with $\Lambda(y = t, t) = 0$. For a given $y \in [0, 0.5)$, $\Lambda(y,t)$ is a linearly increasing function of its second argument t with a slope depending on y as expressed in Eq. (32), a zero minimum obtained at $y = t$, and a maximum achieved for $t = 0.5$ as $\Lambda(y, t = 0.5) = 0.5$.

APPENDIX B
ASYMPTOTIC ANALYSIS OF THE OUTAGE PROBABILITY IN INDEPENDENT CHANNELS

To analyze the asymptotic tendency of the outage probability under independent fading variations, we consider the lossless reconstruction case independently of the lossy case, both at Helper.

A. Lossless Reconstruction at Helper

For any value of the required distortion D_X at Destination, when $D_H = 0$, we have $L_S = H_b(D_H * D_X) - H_b(D_X) = 0$, hence, applying Eq. (24), we obtain $P_{out}^{C_1} = 0$. The system outage probability is then dominated by the second case expressed by

$$\begin{aligned} P_{out} = & P_{out}^{C_2} = \frac{1}{\Gamma_H} \int_{\Phi_H^{-1}(0)}^{\Phi_H^{-1}(1)} \left[\exp\left(-\frac{\gamma_H}{\Gamma_H}\right) \right. \\ & \left. - \exp\left(-\frac{\gamma_H}{\Gamma_H} - \frac{\Phi_S^{-1}(H_S(\gamma_H))}{\Gamma_S}\right) \right] d\gamma_H \end{aligned} \tag{33}$$

Given the power series expansion of the exponential function as $e^{-x} = \sum_{i=0}^{+\infty} \frac{(-x)^i}{i!}$, for small values of x we can use the approximation $e^{-x} \approx 1 - x$. Hence, for high average SNRs, $\Gamma_H, \Gamma_S \to +\infty$, the approximated outage probability reduces to

$$P_{out} \approx \frac{1}{\Gamma_H \Gamma_S} \int_{\Phi_H^{-1}(0)}^{\Phi_H^{-1}(1)} \Phi_S^{-1}\left(H_S(\gamma_H)\right) d\gamma_H \propto \frac{1}{\Gamma_H \Gamma_S},$$

which means that the outage probability asymptotically follows a second-order diversity when $\Gamma_H, \Gamma_S \to +\infty$. We notice that this tendency is also independent of the required distortion D_X at Destination, as long as $D_H = 0$.

B. Lossy Reconstruction at Helper

When the source distortion achieved at Helper is $D_H \neq 0$, we can conclude from Eqs. (24) and (25) that when $\Gamma_H, \Gamma_S \to +\infty$, the outage probability will be dominated by the first case as $P_{out}^{C_2} \to 0$. Hence, the outage probability can be approximated as:

$$P_{out} \approx P_{out}^{C_1} = 1 - \exp\left(\frac{-\Phi_S^{-1}(L_S)}{\Gamma_S}\right), \tag{34}$$

which, using the exponential function approximation, reduces to

$$P_{out} \approx \frac{\Phi_S^{-1}(L_S)}{\Gamma_S} \propto \frac{1}{\Gamma_S}, \tag{35}$$

when $\Gamma_S \to +\infty$. This result shows that for any value of D_X, as long as $D_H \neq 0$, the outage curve follows the tendency of a first-order diversity.

APPENDIX C
STABILITY ANALYSIS OF NUMERICAL CALCULATIONS BY THE TAYLOR SERIES EXPANSION

Since the integral of Eqs. (27) and (28) can be rewritten as

$$\begin{aligned} & \left(\frac{\gamma_S \gamma_H}{\Gamma_S \Gamma_H}\right)^m \exp\left(-a\frac{\gamma_S}{\Gamma_S}\right) \exp\left(-a\frac{\gamma_H}{\Gamma_H}\right) \\ = & \frac{\Gamma_S \Gamma_H}{a^{2(m+1)}} \left(\frac{\gamma_S^m}{(\Gamma_S/a)^{m+1}}\right) \left(\frac{\gamma_H^m}{(\Gamma_H/a)^{m+1}}\right) \\ & \cdot \exp\left(-\frac{\gamma_S}{\Gamma_S/a}\right) \exp\left(-\frac{\gamma_H}{\Gamma_H/a}\right) \\ = & \frac{\Gamma_S \Gamma_H (m!)^2}{a^{2(m+1)}} \left(\frac{\gamma_S^m}{m!\,(\Gamma_S/a)^{m+1}}\right) \exp\left(-\frac{\gamma_S}{\Gamma_S/a}\right) \\ & \cdot \left(\frac{\gamma_H^m}{m!\,(\Gamma_H/a)^{m+1}}\right) \exp\left(-\frac{\gamma_H}{\Gamma_H/a}\right) \\ = & \frac{\Gamma_S \Gamma_H (m!)^2}{a^{2(m+1)}} p_{MRC,(m+1)}\left(\gamma_S\right) p_{MRC,(m+1)}\left(\gamma_H\right), \end{aligned} \tag{36}$$

with $p_{MRC,(m+1)}(\gamma), \gamma = \gamma_S$ or γ_H being PDF of the instantaneous SNR gamma after Maximum Ratio Combining with Γ/a being the average SNR for $\Gamma = \Gamma_S$ or Γ_H, as

$$p_{MRC,m}(\gamma) = \frac{1}{(m-1)!} \frac{\gamma^{m-1}}{(\Gamma/a)^m} \exp\left(-\frac{\gamma}{\Gamma/a}\right). \tag{37}$$

Substituting Eqs. (29), (30) into Eq. (36) yields the coefficient of Eq. (36) as

$$\frac{\Gamma_S \Gamma_H (m!)^2}{a^{2(m+1)}} = \frac{1}{A_m} \frac{|\rho|^{2m}}{(1-|\rho|^2)}, \tag{38}$$

resulting in both Eqs. (27) and (28) being

$$\begin{aligned} P_{\text{out}}^{C_1 \text{ or } C_2} = & \sum_{m=0}^{\infty} A_m \int_{h_1}^{h_2} \int_{s_1}^{s_2} \left(\frac{\gamma_S \gamma_H}{\Gamma_S \Gamma_H}\right)^m \exp\left(-a\frac{\gamma_S}{\Gamma_S}\right) \\ & \cdot \exp\left(-a\frac{\gamma_H}{\Gamma_H}\right) d\gamma_S d\gamma_H, \end{aligned} \tag{39}$$

where the boundaries of the integrals are $\{h_1, h_2\} = \{\Phi_H^{-1}(0), \infty\}, \{s_1, s_2\} = \{\Phi_S^{-1}(0), \Phi_S^{-1}(L_S)\}$ for $P_{out}^{C_1}$ and $\{h_1, h_2\} = \{\Phi_H^{-1}(0), \Phi_H^{-1}(1)\}, \{s_1, s_2\} = \{\Phi_S^{-1}(L_S), \Phi_S^{-1}(H_S(\gamma_H))\}$ for $P_{out}^{C_2}$. Eq. (39) can further be expressed as

$$P_{\text{out}}^{C_1 \text{ or } C_2} = \int_{h_1}^{h_2} \int_{s_1}^{s_2} p_{MRC,1}(\gamma_S) p_{MRC,1}(\gamma_H) d\gamma_S d\gamma_H, \quad \text{for } \rho = 0, \tag{40}$$

$$\begin{aligned} P_{\text{out}}^{C_1 \text{ or } C_2} = & \frac{1}{(1-|\rho|^2)} \sum_{m=0}^{\infty} |\rho|^{2m} \int_{h_1}^{h_2} \int_{s_1}^{s_2} p_{MRC,(m+1)}(\gamma_S) \\ & \cdot p_{MRC,(m+1)}(\gamma_H) d\gamma_S d\gamma_H, \text{ for } 0 < \rho < 1, \end{aligned} \tag{41}$$

Obviously since $\rho = 0$ with Eq. (40), it is exactly equivalent to Eqs. (22) and (23) for $P_{\text{out}}^{C_1}$ and $P_{\text{out}}^{C_2}$, respectively, which corresponds to independent fading occurring on the S-D and H-D links. Since with $0 < \rho < 1$ the boundaries for the double integral in Eq. (41) are the same as that for the independent fading case given by Eq. (40), it is found that each term in the summation of Eq. (41) is equivalent to that for calculating $P_{\text{out}}^{C_1}$ and $P_{\text{out}}^{C_2}$, where the PDFs are replaced by that for m-th order MRC diversity $p_{MRC,(m+1)}(\gamma_S)$ and $p_{MRC,(m+1)}(\gamma_H)$. This observation on the commonalty of the double integrals justifies the use of the double integral with the Taylor Series expansion of the Modifies Bessel function. In fact, those outage curves shown in the figures in the previous versions were calculated by the Monte-Carlo method for the double integrals of (40) for $\rho = 0$ and (41) for $0 < \rho < 1$.

Furthermore, since each double integral term in Eq. (41) indicates that the outage probabilities $P_{\text{out}}^{C_1}$ and $P_{\text{out}}^{C_2}$ with the m-th order MRC diversity monotonically decreases as m increases, and since the term $|\rho|^{2m}$ is also monotonically decreasing with m, each term in the summation in Eq. (41), as a whole, also monotonically decreases. Furthermore, since

$$\int_0^\infty \int_0^\infty p_{MRC,(m+1)}(\gamma_S) p_{MRC,(m+1)}(\gamma_H) d\gamma_S d\gamma_H = 1, \quad (42)$$

it is found that the Series of (41) is upper bounded by

$$\begin{aligned} P_{\text{out}}^{C_1 \text{ or } C_2} &= \frac{1}{(1-|\rho|^2)} \sum_{m=0}^{\infty} |\rho|^{2m} \int_{h_1}^{h_2} \int_{s_1}^{s_2} p_{MRC,(m+1)}(\gamma_S) \\ &\qquad \cdot p_{MRC,(m+1)}(\gamma_H) d\gamma_S d\gamma_H \\ &\leq \frac{1}{(1-|\rho|^2)} \sum_{m=0}^{\infty} |\rho|^{2m} \int_{0}^{\infty} \int_{0}^{\infty} p_{MRC,(m+1)}(\gamma_S) \\ &\qquad \cdot p_{MRC,(m+1)}(\gamma_H) d\gamma_S d\gamma_H \\ &\leq \frac{1}{(1-|\rho|^2)} \sum_{m=0}^{\infty} |\rho|^{2m} = \frac{1}{(1-|\rho|^2)^2}. \end{aligned} \quad (43)$$

It can now be concluded that since each term in the summation of Eqs. (27) and (28), or equivalently Eq. (41), is *monotonically decreasing* with m, the summation is *upper bounded* by (43). Hence, the numerical calculation based on the Taylor Series expansion is stable. In fact, the calculations for the plots in Fig. 9 use a convergence test that the calculated value ratio with $m+1$ to with m becomes smaller than, for example, 0.01-0.1, depending on the target outage value range. It is emphasized that only $M \leq 5$ was required.

Appendix D
Asymptotic Tendency Analysis of the Outage Probability in Correlated Channels

In the presence of channel correlation, the joint PDF of the instantaneous SNRs can be written:

$$\begin{aligned} p(\gamma_S, \gamma_H) =& \frac{a}{\Gamma_S \Gamma_H} \exp\left(-a\left(\frac{\gamma_S}{\Gamma_S} + \frac{\gamma_H}{\Gamma_H}\right)\right) \\ &\times I_0\left(2a|\rho|\sqrt{\frac{\gamma_S \gamma_H}{\Gamma_S \Gamma_H}}\right) \end{aligned} \quad (44)$$

with a defined in Eq. (29). With large average SNRs $\Gamma_H, \Gamma_S \to +\infty$, hence the argument of the modified Bessel function tends to be 0, yielding $I_0(0) = 1$. Hence the joint PDF can be further approximated at high SNRs, as:

$$\begin{aligned} p(\gamma_S, \gamma_H) &\approx \frac{a}{\Gamma_S \Gamma_H} \exp\left(-a\frac{\gamma_S}{\Gamma_S}\right) \exp\left(-a\frac{\gamma_H}{\Gamma_H}\right) \\ &= p(\gamma'_S) p(\gamma'_H) \end{aligned} \quad (45)$$

with $\gamma'_S = \frac{\gamma_S}{a}$ and $\gamma'_H = \frac{\gamma_H}{a}$, and their corresponding mean SNRs $\Gamma'_S = \frac{\Gamma_S}{a^2}$ and $\Gamma'_H = \frac{\Gamma_H}{a^2}$ that tend to $+\infty$ when $\Gamma_H, \Gamma_S \to +\infty$. Hence, the outage probability in correlated channels exhibits asymptotically the same tendency as the case of independent channels, for which the tendency, shown in the previous appendix, is mainly depending on the achieved distortion at the helper D_H. Moreover, at high SNRs regime, the achieved diversity order in correlated channels is independent of the destination required distortion D_X, as in the independent channels case.

Acknowledgment

This paper in part includes intellectual results which the first and the last authors achieved when they were with Japan Advanced Institute of Science and Technology (JAIST) but not published yet, and their extensions. This paper submission has been under the permission by JAIST Research Management Section. The first and the last authors highly appreciate for their official permission, especially for the significant efforts made by Mr. Hiroki Seto. The authors would also like to express sincere gratitude to Prof. Fumiyuki Adachi of Tohoku University.

References

[1] Z. Zhang, Y. Xiao, Z. Ma, M. Xiao, Z. Ding, X. Lei, G. K. Karagiannidis, and P. Fan, "6G wireless networks: Vision, requirements, architecture, and key technologies," *IEEE Vehicular Technology Magazine*, vol. 14, no. 3, pp. 28–41, Sep. 2019.

[2] C.-X. Wang, X. You, X. Gao, X. Zhu, Z. Li, C. Zhang, H. Wang, Y. Huang, Y. Chen, H. Haas, J. S. Thompson, E. G. Larsson, M. D. Renzo, W. Tong, P. Zhu, X. Shen, H. V. Poor, and L. Hanzo, "On the road to 6G: Visions, requirements, key technologies, and testbeds," *IEEE Communications Surveys & Tutorials*, vol. 25, no. 2, pp. 905–974, Second quarter 2023.

[3] W. Yang, H. Du, Z. Q. Liew, W. Y. B. Lim, Z. Xiong, D. Niyato, X. Chi, X. Shen, and C. Miao, "Semantic communications for future internet: Fundamentals, applications, and challenges," *IEEE Communications Surveys & Tutorials*, vol. 25, no. 1, pp. 213–250, First quarter 2023.

[4] D. Gündüz, Z. Qin, I. E. Aguerri, H. S. Dhillon, Z. Yang, A. Yener, K. K. Wong, and C.-B. Chae, "Beyond transmitting bits: Context, semantics, and task-oriented communications," *IEEE Journal on Selected Areas in Communications*, vol. 41, no. 1, pp. 5–41, Jan. 2023.

[5] P. Mach and Z. Becvar, "Device-to-device relaying: Optimization, performance perspectives, and open challenges towards 6g networks," *IEEE Communications Surveys & Tutorials*, vol. 24, no. 3, pp. 1336–1393, Third quarter 2022.

[6] J. Wu, T. Yang, D. Wu, K. Kalsi, and K. H. Johansson, "Distributed optimal dispatch of distributed energy resources over lossy communication networks," *IEEE Transactions on Smart Grid*, vol. 8, no. 6, pp. 3125–3137, Nov. 2017.

[7] R. Abu-Aisheh, F. Bronzino, M. Rifai, L. Salaun, and T. Watteyne, "Coordinating a swarm of micro-robots under lossy communication," in *Proceedings of the 19th ACM Conference on Embedded Networked Sensor Systems*, Coimbra, Portugal, Nov. 2021, pp. 635–641.

[8] F. Acciani, P. Frasca, G. Heijenk, and A. A. Stoorvogel, "Stochastic string stability of vehicle platoons via cooperative adaptive cruise control with lossy communication," *IEEE Transactions on Intelligent Transportation Systems*, vol. 23, no. 8, pp. 10 912–10 922, Aug. 2022.

[9] J. Wang, C. Jiang, H. Zhang, Y. Ren, K.-C. Chen, and L. Hanzo, "Thirty years of machine learning: The road to pareto-optimal wireless networks," *IEEE Communications Surveys & Tutorials*, vol. 22, no. 3, pp. 1472–1514, Third quarter 2020.

[10] J. Park, S. Samarakoon, A. Elgabli, J. Kim, M. Bennis, S.-L. Kim, and M. Debbah, "Communication-efficient and distributed learning over wireless networks: Principles and applications," *Proceedings of the IEEE*, vol. 109, no. 5, pp. 796–819, May 2021.

[11] A. Wyner, "On source coding with side information at the decoder," *IEEE Transactions on Information Theory*, vol. 21, no. 3, pp. 294–300, May 1975.

[12] Z. Xiong, A. Liveris, and S. Cheng, "Distributed source coding for sensor networks," *IEEE Signal Processing Magazine*, vol. 21, no. 5, pp. 80–94, Sep. 2004.

[13] D. Slepian and J. Wolf, "Noiseless coding of correlated information sources," *IEEE Transactions on Information Theory*, vol. 19, no. 4, pp. 471–480, Jul. 1973.

[14] X. Zhou, M. Cheng, X. He, and T. Matsumoto, "Exact and approximated outage probability analyses for decode-and-forward relaying system allowing intra-link errors," *IEEE Transactions on Wireless Communications*, vol. 13, no. 12, pp. 7062–7071, Dec. 2014.

[15] J. He, V. Tervo, X. Zhou, X. He, S. Qian, M. Cheng, M. Juntti, and T. Matsumoto, "A tutorial on lossy forwarding cooperative relaying," *IEEE Communications Surveys & Tutorials*, vol. 21, no. 1, pp. 66–87, First quarter 2018.

[16] J. He, V. Tervo, S. Qian, M. Juntti, and T. Matsumoto, "Performance analysis of OSTBC transmission in lossy forward MIMO relay networks," *IEEE Communications Letters*, vol. 21, no. 8, pp. 1791–1794, Aug. 2017.

[17] J. He, V. Tervo, S. Qian, Q. Xue, M. Juntti, and T. Matsumoto, "Performance analysis of lossy decode-and-forward for non-orthogonal MARCs," *IEEE Transactions on Wireless Communications*, vol. 17, no. 3, pp. 1545–1558, Mar. 2018.

[18] S. Qian, V. Tervo, J. He, M. Juntti, and T. Matsumoto, "A comparative study of different relaying strategies over one-way relay networks," in *22th European Wireless Conference*, Oulu, Finland, May 2016, pp. 1–6.

[19] S. Qian, J. He, M. Juntti, and T. Matsumoto, "Fading correlations for wireless cooperative communications: Diversity and coding gains," *IEEE Access*, vol. 5, pp. 8001–8016, Apr. 2017.

[20] G. Lin, Y. Zhou, W. Jiang, X. He, X. Zhou, G. He, and P. Yang, "LF-SWIPT: Outage analysis for SWIPT relaying networks using lossy forwarding with QoS guaranteed," *IEEE Internet of Things Journal*, vol. 9, no. 19, pp. 18 737–18 748, Oct. 2022.

[21] Y. Ye, L. Shi, X. Chu, H. Zhang, and G. Lu, "On the outage performance of SWIPT-based three-step two-way DF relay networks," *IEEE Transactions on Vehicular Technology*, vol. 68, no. 3, pp. 3016–3021, Mar. 2019.

[22] M. Cheng and X. Meng, "Decode-and-forward vs. lossy-forward: Intelligent reflecting surface-assisted sidelink transmission," *IEEE Transactions on Vehicular Technology*, vol. 72, no. 9, pp. 12 425–12 429, Sep. 2023.

[23] A. Wyner and J. Ziv, "The rate-distortion function for source coding with side information at the decoder," *IEEE Transactions on information Theory*, vol. 22, no. 1, pp. 1–10, Jan. 1976.

[24] T. Berger, "Multiterminal source coding," in *The Information Theory Approach to Communications, G. Longo, Ed.* New York: Springer-Verlag, 1978, pp. 171–231.

[25] S. Y. Tung, "Multiterminal source coding," Ph.D. dissertation, School of Electrical Engineering, Cornell University, Ithaca, New York, 1978.

[26] Y. Oohama, "The rate-distortion function for the quadratic Gaussian CEO problem," *IEEE Transactions on Information Theory*, vol. 44, no. 3, pp. 1057–1070, May 1998.

[27] H. Yang, T. Ding, and X. Yuan, "Federated learning with lossy distributed source coding: Analysis and optimization," *IEEE Transactions on Communications*, vol. 71, no. 8, pp. 4561–4576, Aug. 2023.

[28] W. Lin, S. Qian, and T. Matsumoto, "Lossy-forward relaying for lossy communications: Rate-distortion and outage probability analyses," *IEEE Transactions on Wireless Communications*, vol. 18, no. 8, pp. 3974–3986, Aug. 2019.

[29] S. Song, J. He, and T. Matsumoto, "Rate-distortion and outage probability analyses of Wyner-Ziv systems over multiple access channels," *IEEE Transactions on Communications*, vol. 69, no. 9, pp. 5807–5816, Sep. 2021.

[30] W. Lin, Q. Xue, J. He, M. Juntti, and T. Matsumoto, "Rate-distortion and outage probability analyses for single helper assisted lossy communications," *IEEE Transactions on Vehicular Technology*, vol. 68, no. 11, pp. 10 882–10 894, Nov. 2019.

[31] W. Lin, L. Li, J. Yuan, Z. Han, M. Juntti, and T. Matsumoto, "Cooperative lossy communications in unmanned aerial vehicle networks: Age-of-information with outage probability," *IEEE Transactions on Vehicular Technology*, vol. 70, no. 10, pp. 10 105–10 120, Oct. 2021.

[32] ——, "Age-of-information in first-come-first-served wireless communications: Upper bound and performance optimization," *IEEE Transactions on Vehicular Technology*, vol. 71, no. 9, pp. 9501–9515, Sep. 2022.

[33] J. Garcia-Frias and Y. Zhao, "Near-Shannon/Slepian-Wolf performance for unknown correlated sources over AWGN channels," *IEEE Transactions on Communications*, vol. 53, no. 4, pp. 555–559, Apr. 2005.

[34] H. Omori, T. Asai, and T. Matsumoto, "A matched filter approximation for SC/MMSE iterative equalizers," *IEEE Communications Letters*, vol. 5, no. 7, pp. 310–312, Jul. 2001.

[35] A. Goldsmith, *Wireless Communications*. Cambridge university press, 2005.

[36] S. Song, M. Cheng, J. He, X. Zhou, and T. Matsumoto, "Outage probability of one-source-with-one- helper sensor systems in block Rayleigh fading multiple access channels," *IEEE Sensors Journal*, vol. 21, no. 2, pp. 2140–2148, Jan. 2021.

[37] A. Barbu and S.-C. Zhu, *Monte Carlo Methods*. Singapore: Springer, 2020.

[38] T. M. Cover and J. A. Thomas, *Elements of Information Theory*, 2nd ed. John Wiley & Sons, 2012.

[39] R. Youssef and A. G. i. Amat, "Distributed serially concatenated codes for multi-source cooperative relay networks," *IEEE Transactions on Wireless Communications*, vol. 10, no. 1, pp. 253–263, Jan. 2011.

[40] C. Chen, M. Shu, Y. Wang, and N. Wei, "A study on the second order statistics of κ-μ fading channels," in *Wireless Algorithms, Systems, and Applications*, L. Ma, A. Khreishah, Y. Zhang, and M. Yan, Eds. Guilin, China: Springer International Publishing, Jun. 2017, pp. 559–571.

[41] A. A. Kilbas and M. Saigo, *H-Transforms: Theory and Applications*. Florida: CRC Press, 2004.

[42] M. Cheng, K. Anwar, and T. Matsumoto, "Outage probability of a relay strategy allowing intra-link errors utilizing Slepian-Wolf theorem," *EURASIP Journal on Advances in Signal Processing*, vol. 2013, pp. 1–12, Feb. 2013.

[43] G. N. Watson, *A Treatise on the Theory of Bessel Functions*. Cambridge, UK: Cambridge University Press, 1944.